JOURNAL OF CATALYSIS 20, 141-146 (1971)

Hydrogen–Deuterium Exchange on Zinc Oxide

R. TARTARELLI, M. GIORGINI, AND F. MORELLI

Institute of Industrial and Applied Chemistry, Pisa University, Italy

Received February 26, 1970; revised July 20, 1970

The hydrogen-deuterium exchange on zinc oxide has been studied from 100 to 160°C. The first order reaction rate constant above a certain temperature is strongly influenced by the catalyst particle size and three different activation energies are observed on the Ärrhenius plot with the increase of temperature: 52, 9.9, and 28 kcal/mole, respectively. The experimental results have been interpreted on the grounds of diffusion effects within the particle and a branched-pore structure of the catalyst is proposed.

Smith and Taylor (*1*) studied the hydrogen–deuterium exchange on zinc oxide and used surface heterogeneity to explain an abnormal temperature coefficient in the temperature range where a transition between two types of adsorption has been revealed (*2*). In fact, in the interval 132–157°C no change in the reaction rate was found, and the activation energies, outside this temperature range, fell into three groups: 0.6 and 4.9 kcal/mole below −78°C, 7–8 kcal/mole from −78 to 100°C and 11–13 kcal/mole above this temperature.

On the contrary Holm and Blue (*3*) obtained a normal temperature coefficient throughout a temperature range including the region 132–157°C and attributed the low temperature coefficients reported by Smith and Taylor (*1*), to a loss of catalyst activity during the tests.

The interest of Molinari and Parravano (*4, 5*) in studying the hydrogen–deuterium exchange on sintered and unsintered zinc oxide lays in a connection between catalytic activity and semiconductivity, which last was modified by suitable addition of foreign ions to the catalyst. The Ärrhenius plot of the kinetic data did not yield straight lines in the temperature range covered (*6*). For all the sintered catalysts above a temperature in the neighborhood of 115°C, the apparent activation energy became very low, and above the temperature range of practically zero activation energy, a temperature coefficient was obtained as large as before. The unsintered catalysts, which were activated in hydrogen, gave straight lines on the Ärrhenius plot from 25 to 185°C or more. The variations in the activation energy with temperature were attributed to the presence of two hydrogenated compounds (*7*).

A mechanism of induced desorption has been proposed by Molinari (*8*) to explain changes in activation energy.

Unfortunately, in the above references the effect of the catalyst sizes was not taken into due account to determinate whether or not the reaction rate is limited by intraparticle diffusion. It is well known that the apparent activation energy of a reaction process is lowered by the occurrence of diffusional resistances, to which the abnormal temperature coefficients observed in the hydrogen–deuterium exchange might be ascribed. In the present paper the marked effect of the particle size on the reaction rate above a certain temperature is reported and the variations of the activation energy with temperature are discussed and interpreted on the grounds of a catalyst multibranched-pore model.

EXPERIMENTAL METHODS

The zinc oxide was prepared by thermal decomposition of oxalate (zinc nitrate and ammonium oxalate molar solutions) (*9*).

The zinc oxalate precipitate, washed until free of nitrates, had been calcined for 14 hr in a current of nitrogen and the zinc oxide powder had been sintered at 300°C for 3 hr under a 230 kg/cm^2 pressure. The catalyst pills were broken up into small pieces which were separated by DIN 1171 series sieves into a number of size fractions. Before employment, the catalyst was kept in an oven at 450°C for 6 hr and activated at 300°C in the reactor for 9 hr in a current of hydrogen (flow rate $\simeq 1$ liter/hr).

The surface area (BET) of the catalyst pellets, previously kept at 450°C for 6 hr, was measured by a Carlo Erba Sorptomatic apparatus. The different sized particles had, practically, the same surface area, whose value was about 13.5 m^2/g (*10*). The pore size distribution and adsorption and desorption isotherms of the catalyst pellets are reported elsewhere (*10*).

The kinetics of the hydrogen–deuterium reaction was followed in a flow system. A stream of H_2 containing D_2 and HD (the composition of the gas mixture feed, which at the start of the present research was 98% H_2 and 2% D_2, due to the extent of reaction in the bottle changed to 97.6% H_2, 1.6% D_2 and 0.8% HD at the end) flowed at atmospheric pressure through the catalyst into a 5 mm diameter Pyrex glass tube electrically heated reactor, temperature of which was controlled by a thermocouple positioned in the catalyst (±0.1°C). For analyzing the reacted mixture, the reactor was coupled to a Carlo Erba Mod. C thermal conductivity detector chromatographic apparatus which was operated as follows: Column: 1m in length and 5 mm in diameter filled with Carlo Erba 0.85L Alumina which had been activated for 12 hr at 250°C in a current of helium; column temperature: −197°C, hydrogen flow rate: 3 liter/hr.

The kinetic data have been computed from the equation:

$$\ln \frac{\chi_e - \chi_i}{\chi_e - \chi_f} = \frac{K\tau}{\chi_e} \qquad (1)$$

where χ is the conversion of D_2 to HD (χ_i = conversion in the gas bottle, χ_f = conversion at the exit of the reactor), K the rate of exchange and τ the spatial time defined as ratio between catalyst weight and volumetric feed rate. χ_e denotes the equilibrium conversion of D_2 in the $H_2 +$ 2% D_2 mixture; its temperature dependence is negligible (*11*, *12*). The Equation (1) follows from the first-order kinetics of the exchange reaction (*1*, *5*, *6*, *12*). The activation energies of the process can be obtained from the Årrhenius plot of

$$\frac{\chi_e}{\tau} \ln \frac{\chi_e - \chi_i}{\chi_e - \chi_f}.$$

RESULTS

To determinate whether or not film diffusion has taken place, two series of runs have been made at varying values of τ with a constant weight of catalyst in each run series. The two curves, which are plotted in Fig. 1 with

$$\ln \frac{\chi_e - \chi_i}{\chi_e - \chi_f}$$

vs τ at two reaction temperatures for a 14–23 mesh catalyst, coincide in the range of experimented values of τ; therefore, there is no film diffusion effect. In addition, the first-order kinetics of the exchange reaction is supported by the present data.

The rate of exchange is reported in Fig. 2 on the Årrhenius plot for various catalyst sizes (the temperature range has been explored with both rising and decreasing

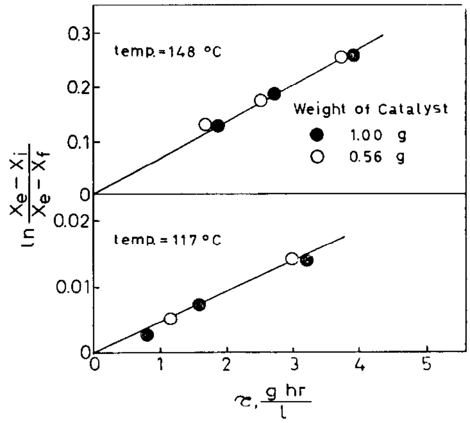

FIG. 1. Conversion versus spatial time with two weights of 14–23 mesh catalyst. Film diffusion is not limiting.

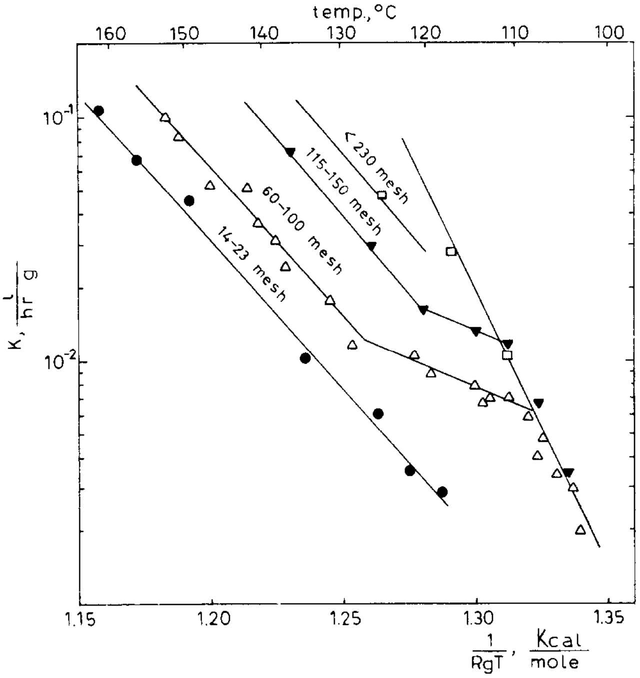

FIG. 2. Årrhenius plot for various sized catalyst pellets.

temperature without revealing any evidence of catalyst deactivation during the runs). It is plain that the size of particle plays a marked role on the reaction rate, showing a pore diffusion effect through the catalyst pellet. Moreover, three ranges of temperature characterized by different values of activation energy may be recognized, in agreement with the data of Smith and Taylor (*1*) and Molinari and Parravano (*4*). The observed activation energy is 52 kcal/mole in the first range of temperature, then it drops to 9.9 kcal/mole in the second. Above a certain temperature, the exchange picks up speed again showing an activation energy of 28 kcal/mole. The curves of the different sizes of particles overlap in the first range of temperature and the break which follows it occurs at the higher temperatures as the size of the catalyst particle decreases. The runs were stopped at the temperature where film diffusion effects became evident.

DISCUSSION

The present data indicate the strong effect of the size of particle on the exchange rate. Consequently, it becomes hard for us to attribute the breaks in the Årrhenius plot exclusively to two types of adsorption or to two different hydrogenated compounds or to an induced desorption mechanism. In fact, on the last grounds the variation in the activation energy should be occurring at a certain temperature independently of the size of particle. Furthermore, the straight-line Årrhenius plots, previously obtained (*3*, *4*), do not agree very well with the proposed mechanisms. Rather, an interpretation based on diffusion effects within the catalyst may be given.

As the reaction rate, at low temperature, is independent of the size of particle, the reaction step on the surface of the catalyst is controlling. With increasing the temperature, the diffusional resistances within the particle become increasingly important relative to the resistance to chemical step until strong pore diffusion regime appears and the apparent activation energy approaches a minimum value if no film diffusion effects are involved (*13*, *14*).

In the present investigation the chemical regime can be considered falling in the first range of temperature, where all the curves in Fig. 2 overlap and 52 kcal/mole is the activation energy of the reaction step. The successive decrease of the observed activation energy from 52 to 9.9 kcal/mole may be attributed to the occurrence of the strong pore diffusion regime. In the last conditions (the catalyst particle may be considered isothermal), as reported in Appendix the ratio between the apparent activation energy and the true activation energy is related to the branching degree of the porous structure, α, by the equation:

$$\frac{E_{\mathrm{app}}}{E_0} = \frac{1}{2^\alpha}. \tag{2}$$

The experimental data of Fig. 2 give $\alpha \simeq 2.4$; on this value an intermediate pore model between a two-branched and a three-branched one may be proposed to schematize the porous structure of the zinc oxide pellets. As concerns the catalyst structure, the classical single-pore model (*15, 16*) has been extended by Mingle and Smith (*17*) and Carberry (*18, 19*), who introduced the macro-micropore model to represent catalyst pills containing macropores, created via pelleting of porous microspheres. The last model may be visualized by a cylindrical pore (macropore) from which micropores branch along the length and at right angle to the macropore (two-branched pore model). A three-branched-pore model is generated from the previous one via branching of micropores along the length and at right angle from the existing micropores; therefore, the experimental value of α, obtained on a sintered catalyst, may be considered physically consistent. The successive increase of the observed activation energy from 9.9 to 28 kcal/mole may be attributed to the increasing limitation of the diffusion–reaction zone at the outer surface of the particle where branched pores are not involved. Hence, in this temperature range, a value $\alpha \simeq 0.9$ is obtained, which practically conforms to the single-pore model.

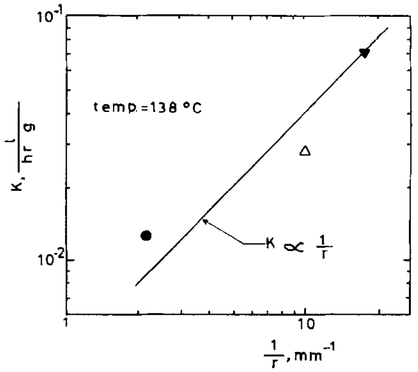

FIG. 3. Exchange rate versus arithmetic-mean-radius of catalyst pellet.

With a further increase of temperature, when the reaction process is limited at the external surface of the particle, an activation energy of 52 kcal/mole must be expected again (pseudochemical regime). In the present case these conditions cannot be achieved because the range of temperature investigated is limited by the occurrence of film fluid resistances. Nevertheless, Smith and Taylor (*1*) and Molinari and Parravano (*4, 6*) after the temperature range of very low activation energy, obtained a temperature coefficient as large as before. The dependence of the exchange rate on the particle-arithmetic-mean radius, reported in Fig. 3, appears to support such standpoint in the interpretation of the experimental results. Deviations from the theoretical behavior may be attributed to irregularity of the catalyst particles.

SUMMARY

The rate of the reaction $H_2 + D_2 = 2$ HD on zinc oxide has been studied from 100 to 160°C, and the reaction shown to be first order.

The size of catalyst particle above a certain temperature plays a marked role on the reaction rate revealing a pore diffusion effect within the catalyst particle.

Three successive ranges of temperatures have been recognized where the activation energy is 52, 9.9, and 28 kcal/mole, respectively. The break of the activation energy from 52 to 9.9 kcal/mole is interpreted as a transition from a chemical regime to a strong pore diffusion one. The following increase of the activation energy from 9.9 to 28 kcal/mole is attributed to the increasing limitation of the diffusion–reaction zone at

the outer surface of the particle where branched pores are not involved.

From the ratio between the observed activation energy in strong pore diffusion regime and the true activation energy, evaluated in the chemical regime, the branching degree of the porous structure has been calculated, assuming a multi-branched-pore model.

APPENDIX

Let us consider the reaction:

$$C + A \rightleftarrows 2B \qquad (\mathrm{A}.1)$$

with first-order reversible kinetics:

$$r_s = K_1[A] - K_2[B]. \qquad (\mathrm{A}.2)$$

In the α-branched-pore model, call ith-pores those of the ith-branching; let the ith-pores have radius r_i and length l_i and the diffusivity within be the same for both the reactants A and B. Assume the surface of (i-1)th-pore entirely covered by ith-pores. From the stoichiometry of the reaction (A.1) the reduced concentration of B may be related to the reduced concentration of A by the equation:

$$b_i = -2a_i + 2a_0 + b_0. \qquad (\mathrm{A}.3)$$

The α-material balance equations are

$$(\alpha\text{th-pores})\ \frac{d^2a_\alpha}{d\rho_\alpha{}^2} = \frac{m_\alpha{}^2}{2\chi_e} \times [2a_\alpha - (1-\chi_e)(2a_0+b_0)] \qquad (\mathrm{A}.4)$$

and

$$(j\text{th-pores})\ \frac{d^2a_j}{d\rho_j{}^2} = 2\theta_j{}^2\left(-\frac{da_{j+1}}{d\rho_{j+1}}\right)_{\rho_{j+1}} = 0, \qquad (\mathrm{A}.\alpha - j + 4)$$

$1 \leqslant j \leqslant \alpha - 1$

where

$$m_\alpha \equiv \left(\frac{2K_1}{r_\alpha D_\alpha}\right)^{1/2} l_\alpha$$

is the αth-pore diffusion reaction modulus and

$$\theta_j \equiv \left(\frac{D_{j+1}}{D_j}\,\frac{l_j{}^2}{r_j l_{j+1}}\right)^{1/2}$$

are the geometric moduli of the multi-branched porous structure.

In strong pore diffusion regimes the reaction rate drops to zero at the pore ends where the equilibrium conditions are established.

By solving the Eqs. (A.4) and (A.$\alpha + 3$), the rate of transport of reactant A into the pore is obtained:

$$\phi_\alpha = 2^{1-1/2^{\alpha-1}}\frac{\pi r_1{}^2 D_1}{l_1}\left(\prod_{h=1,\ldots,\alpha-1}\theta_h{}^{1/2^{h-1}}\right) \times \left(\frac{m_\alpha}{\sqrt{\chi_e}}\right)^{1/2^{\alpha-1}}[A]_0{}^0(\chi_e - \chi).$$

The material balance of A for a differential element of weight of catalyst (the catalyst pellets are considered spheres) in a plug flow reactor is

$$v_0[A]_0{}^0\,d\chi = \frac{3\epsilon}{\pi r_1{}^2 d}\,\frac{1}{r}\,\phi_\alpha\,dP. \qquad (\mathrm{A}.\alpha + 5)$$

Integration of Eq. (A.$\alpha + 5$) gives

$$\ln\frac{\chi_e - \chi_i}{\chi_e - \chi_f} = K\frac{P}{\chi_e v_0} \qquad (\mathrm{A}.\alpha + 6)$$

with

$$K \equiv \frac{3 \times 2^{1-1/2^{\alpha-1}}\epsilon D_1}{dl_1}\left(\prod_{h=1,\ldots,\alpha-1}\theta_h{}^{1/2^{h-1}}\right) \times \left(\frac{m_\alpha}{\sqrt{\chi_e}}\right)^{1/2^{\alpha-1}}\chi_e\frac{1}{r}. \qquad (\mathrm{A}.\alpha + 7)$$

If the temperature dependence of both diffusivity and χ_e is negligible, the apparent activation energy, defined as

$$E_{\mathrm{app}} \equiv -\frac{\partial \ln K}{\partial(1/R_gT)},$$

in diffusion-limited regimes becomes:

$$\frac{E_{\mathrm{app}}}{E_0} = \frac{1}{2^\alpha}. \qquad (\mathrm{A}.\alpha + 8)$$

In the same conditions, the dependence of reaction rate on radius of catalyst particle is expressed by:

$$\frac{\partial \ln K}{\partial \ln (1/r)} = 1. \qquad (\mathrm{A}.\alpha + 9)$$

ACKNOWLEDGMENTS

We thank the Italian Consiglio Nazionale delle Ricerche for financial aid.

REFERENCES

1. SMITH, C. A., AND TAYLOR, H. S., *J. Amer. Chem. Soc.* **60,** 362 (1938).
2. TAYLOR, H. S., AND STROTHER, C. O., *J. Amer. Chem. Soc.* **50,** 586 (1934).
3. HOLM, V. C., AND BLUE, R. W., *Ind. Eng. Chem.* **44,** 107 (1952).
4. MOLINARI, E., AND PARRAVANO, G., *J. Amer. Chem. Soc.* **75,** 5233 (1953).
5. MOLINARI, E., *Gazz. Chim. Ital.* **85,** 930 (1955).
6. PARRAVANO, G., AND BOUDART, M., *Adv. Catal. Rel. Subj.* **7,** 47 (1955).
7. WICKE, E., *Z. Elektrochem.* **53,** 279 (1949).
8. MOLINARI, E., *Z. physik. Chem. Frankfurt am Main* **6,** 1 (1956).
9. TAYLOR, H. S., AND SICKMAN, D. V., *J. Amer. Soc.* **54,** 602 (1932).
10. SBRANA, F., Chem. Engng. Thesis, University of Pisa, 1969.
11. UREY, H. C., AND RITTENBERG, D., *J. Chem. Phys.* **1,** 137 (1933).
12. SHIGEHARA, Y., AND OZAKI, A., *J. Catal.* **10,** 183 (1968).
13. BACCAREDDA, M., TARTARELLI, R., MORELLI, F., GIORGINI, M., AND LUCCHESI, A., *Proc. Int. Congr. Catal., 4, 1968.*
14. CALVELO, A., AND CUNNINGHAM, R. E., *J. Catal.* **16,** 397 (1970).
15. THIELE, E. W., *Ind. Eng. Chem.* **31,** 916 (1939).
16. ZELDOVICH, J. B., *Z. Fiz. Khim* **13,** 163 (1939).
17. MINGLE, J. O., AND SMITH, J. M., *Amer. Inst. Chem. Eng. J.* **7,** 243 (1961).
18. CARBERRY, J. J., *Amer. Inst. Chem. Eng. J.* **8,** 557 (1962).
19. CARBERRY, J. J., *Chem. Eng. Sci.* **17,** 675 (1962).